An Imager's Guide to Perineural Tumor Spread in Head and Neck Cancers: Radiologic Footprints on ^{18}F-FDG PET, with CT and MRI Correlates

Hwan Lee[1], Jillian W. Lazor[2], Reza Assadsangabi[1], and Jagruti Shah[1]

[1]*Division of Nuclear Medicine and Clinical Molecular Imaging, Department of Radiology, University of Pennsylvania, Philadelphia, Pennsylvania; and* [2]*Division of Neuroradiology, Department of Radiology, University of Pennsylvania, Philadelphia, Pennsylvania*

Learning Objectives: On successful completion of this activity, participants should be able to (1) describe the neural pathways and basic anatomy of the commonly involved cranial nerves with perineural spread of tumor; (2) recognize the imaging findings of perineural spread in head and neck cancers on functional and anatomic imaging; and (3) explain the definition, pathogenesis, and clinical significance of perineural spread.

Financial Disclosure: The authors of this article have indicated no relevant relationships that could be perceived as a real or apparent conflict of interest.

CME Credit: SNMMI is accredited by the Accreditation Council for Continuing Medical Education (ACCME) to sponsor continuing education for physicians. SNMMI designates each *JNM* continuing education article for a maximum of 2.0 AMA PRA Category 1 Credits. Physicians should claim only credit commensurate with the extent of their participation in the activity. For CE credit, SAM, and other credit types, participants can access this activity through the SNMMI website (http://www.snmmilearningcenter.org) through March 2022.

Perineural spread (PNS) refers to tumor growth along large nerves, a macroscopic analog of microscopic perineural invasion. This phenomenon most commonly occurs in the head and neck, but its incidence varies with histologic tumor subtype. PNS results from a complex molecular interplay between tumor cells, nerves, and connective stroma. PNS is clinically underdiagnosed despite its impact on patients' prognosis and management. The role of ^{18}F-FDG PET in assessment of PNS in head and neck cancer remains to be explored, in contrast to MRI as the established gold standard. In patients with PNS, ^{18}F-FDG PET shows both abnormality along the course of the involved nerve and muscular changes secondary to denervation. Assessment of PNS on ^{18}F-FDG PET requires knowledge of relevant neural pathways and can be improved by correlation with anatomic imaging, additional processing of images, and review of clinical context.

Key Words: perineural spread; head and neck cancer; cranial nerves; ^{18}F-FDG PET; correlative imaging

J Nucl Med 2019; 60:304–311
DOI: 10.2967/jnumed.118.214312

The term *head and neck cancer* encompasses a heterogeneous group of malignancies occurring in the oral, sinonasal, pharyngeal, and laryngeal mucosa, as well as in the salivary glands and skin of the head and neck (*1*). Diagnosis and management of head and neck cancer often involve ^{18}F-FDG PET/CT imaging for a variety of roles, including detection of an unknown primary tumor, staging, radiation therapy planning, response assessment, and posttreatment surveillance (*2*).

Received Jul. 3, 2018; revision accepted Sep. 26, 2018.
For correspondence or reprints contact: Jagruti Shah, University of Pennsylvania, 3400 Spruce St., Donner 110 A, Philadelphia, PA 19104.
E-mail: jagruti.shah4@gmail.com
Published online Oct. 5, 2018.
COPYRIGHT © 2019 by the Society of Nuclear Medicine and Molecular Imaging.

Head and neck cancer can spread by direct extension or by hematogenous or lymphatic routes (*3*). An additional means of spread is extension of tumor along nerves, a phenomenon called perineural tumor growth (*3*). Imaging is critical in diagnosis of perineural tumor growth: clinical underdiagnosis is common because up to 40% of the affected patients are asymptomatic (*4*).

Although the sensitivity and specificity of MRI in assessment of perineural tumor growth have been characterized (*5–7*), there are limited data on the accuracy of ^{18}F-FDG PET in detecting perineural tumor growth (*3*). The aim of this article is to increase awareness of perineural spread (PNS) in head and neck cancer and describe imaging findings of PNS with a focus on ^{18}F-FDG PET. We summarize the pathogenesis, clinical implications, and pattern of PNS, with emphasis on neuroanatomy and primary and secondary imaging findings of PNS on both metabolic and anatomic imaging.

DEFINITION AND INCIDENCE

Extension of neoplasia along the course of a nerve is termed perineural tumor growth, which is divided into 2 types: perineural invasion (PNI) and PNS. PNI refers to tumor invasion into the neural space of small, unnamed nerve branches confined to the main tumor site, whereas PNS involves larger, named nerves often accompanied by distant tumor spread along the nerves away from the primary site (*8*). Unlike PNI, PNS is evident on imaging and can be discovered by clinical manifestations directly related to the involved nerve (*7*).

Most of the available data on the incidence and prevalence of perineural growth of head and neck tumors refer to PNI rather than PNS. Regardless of the choice of terminology, a relative comparison of the propensity for nerve involvement among different histologic tumor types remains informative.

The overall reported incidence of PNI in head and neck cancers varies widely, from 2.5% to 80%, because frequency varies with the tumor histologic type and the location of the primary tumor (*9,10*). The rates of PNI for various histologic types are summarized in Supplemental Table 1 (supplemental materials are available at

http://jnm.snmjournals.org) (*11–23*). The risk for PNS is higher if the tumor is recurrent, large, at a midface location, or poorly differentiated and if the patient is male (*24*). The evaluation and interpretation of suspected imaging findings of PNS can be improved by accounting for the histologic type and the location of the primary tumor and by carefully evaluating certain anatomic sites that are more conducive to neural involvement, such as the masticator space, pterygopalatine fossa, Meckel cave, and cavernous sinus (*3,10,25,26*).

PATHOGENIC MECHANISM

The most current and widely accepted model of perineural tumor growth is based on a complex biochemical interaction between the tumor cells and the nerve microenvironment (*8*). The functional outcomes of the biochemical interactions include stromal manipulation, neurotropism, neurite production, and nerve–tumor adhesion (Fig. 1) (*8,27*). To date, several proteins have been discovered to play a role (Fig. 1). The full biochemical landscape remains to be explored, with ongoing discovery of an increasing number of mechanisms, such as nerve-initiated immune response (*28*).

Differences in the biochemical profile of tumors can explain the variation in their propensity for perineural growth. For example, desmoplastic melanoma, a type of melanoma with high rates of PNI (Supplemental Table 1), exhibits higher expression of nerve growth factor receptor, a protein involved in PNS (*29*). Continued research on the pathogenesis of perineural tumor growth can lead to potential therapeutic targets. For example, blockade of tropomyosin receptor kinases, involved in PNS signaling (*30*), has reached a phase II clinical trial with promising results in patients with various tumor types, including head and neck cancers (*31*).

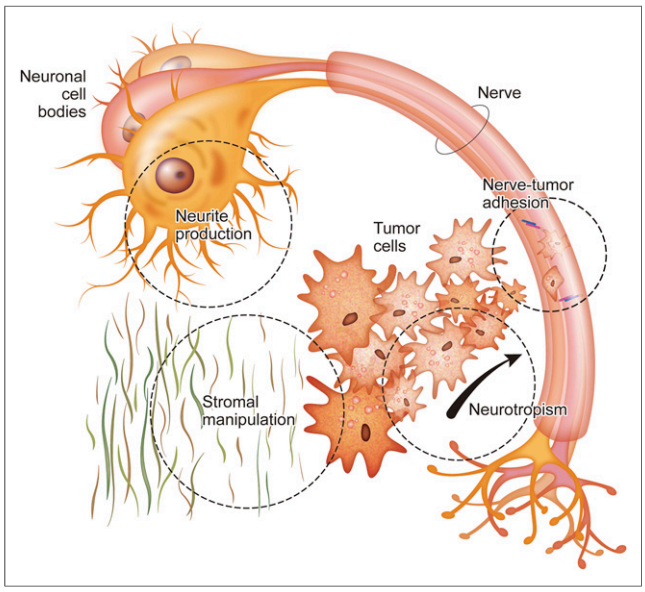

FIGURE 1. Functional outcomes of biochemical mechanisms involved in perineural tumor growth. Connective stroma surrounding tumor cells is manipulated to facilitate perineural tumor spread, for example by matrix metalloproteinases. Nerve-tumor adhesion is achieved by membrane proteins such as neural cell adhesion molecule. Activation of nuclear transcription factors by various signaling molecules, including nerve growth factor, brain-derived neurotrophic factor, glial cell-line–derived neurotrophic factor, neurotrophin-3, and neurotrophin-4, contributes to stromal manipulation and nerve-tumor adhesion. It also leads to homing of tumor cells to nerves (neurotropism) and production of neurites to increase nerve-tumor contact (*8,27*).

CLINICAL SIGNIFICANCE

Perineural involvement of tumor affects prognosis, risk stratification, staging, and treatment planning. The prognostic value of perineural involvement varies with the histologic subtype of the tumor and the site of the primary malignancy. In general, perineural disease confers a higher risk of local recurrence, a higher risk of metastasis, and poorer survival.

In mucosal head and neck squamous cell carcinoma (all subsites), PNI is associated with increased local recurrence (23% vs. 9%) and worse disease-specific mortality (54% vs. 25%) (*32*). PNI has also been found to be a predictor of lymph node metastases (*32*). PNI is a predictor of distant recurrence and worse disease-free survival in oral tongue squamous cell carcinoma (*33*). In cutaneous head and neck squamous cell carcinoma with PNI, the rate of 10-y local control is significantly worse in symptomatic patients than in asymptomatic patients (50% vs. 78%) (*24*).

Poor prognosis has been observed in salivary gland cancers with PNI. In patients with mucoepidermoid carcinoma, PNI was associated with a decreased 5-y disease-free survival (57.7% vs. 88.8%) (*17*). In adenoid cystic carcinoma, PNI was associated with a higher rate of recurrence (81.8% vs. 26.7%), a higher rate of distant metastases (40% vs. 0%), and lower 5-y survival (36.9% vs. 93.8%) (*34*).

Fewer studies have explored the prognostic implications of PNS as detected on imaging. Williams et al. found that patients with cutaneous squamous cell and basal cell carcinoma with and without PNS on imaging had significantly worse 5-y local control rates (35% vs. 78%), 5-y overall survival (50% vs. 86%), and 5-y cause-specific survival (54% vs. 94%) (*35*). Balamucki et al. found a significant difference in 5-y disease-specific survival in patients with and without radiographic evidence of PNS in cutaneous head and neck squamous cell carcinoma (*24*).

These prognostic implications are important for clinical management and treatment planning. With regard to the site of the primary tumor, the goal of surgical excision is complete resection of tumor and the involved extracranial nerve. Intracranial extension of PNS deems a patient inoperable because of the risk of tumor seeding into the central nervous system. These patients are often treated with palliative radiation (*36*) or with surgery performed on a case-by-case basis with the goal of tumor debulking to improve the efficacy of adjuvant therapy and reduce symptoms (*37*). The 2018 National Comprehensive Cancer Network guidelines recommend postsurgical adjuvant radiation for mucosal head and neck squamous cell carcinoma, salivary gland carcinoma, and melanoma with PNI (*38,39*), as well for cutaneous squamous cell and basal cell carcinoma with extensive or large-nerve PNI (*40,41*).

PERINEURAL PATHWAYS

PNS in head and neck cancers can occur along any cranial nerve (CN). The most commonly involved CNs in PNS are the maxillary and mandibular division of the trigeminal nerve (CNs V2 and V3, respectively) and the facial nerve (CN VII) because of their widespread innervation of the head and neck structures (*1*). The ophthalmic division of the trigeminal nerve (CN V1) and the hypoglossal nerve (CN XII) are less frequently involved (*10*). Primary tumor sites for the CNs commonly involved in PNS are summarized in Supplemental Table 2.

Tumors may spread from one CN to another because of their close proximity to one another or because of communication between their peripheral branches, particularly between CNs V and VII. There are at least a few different locations at which they

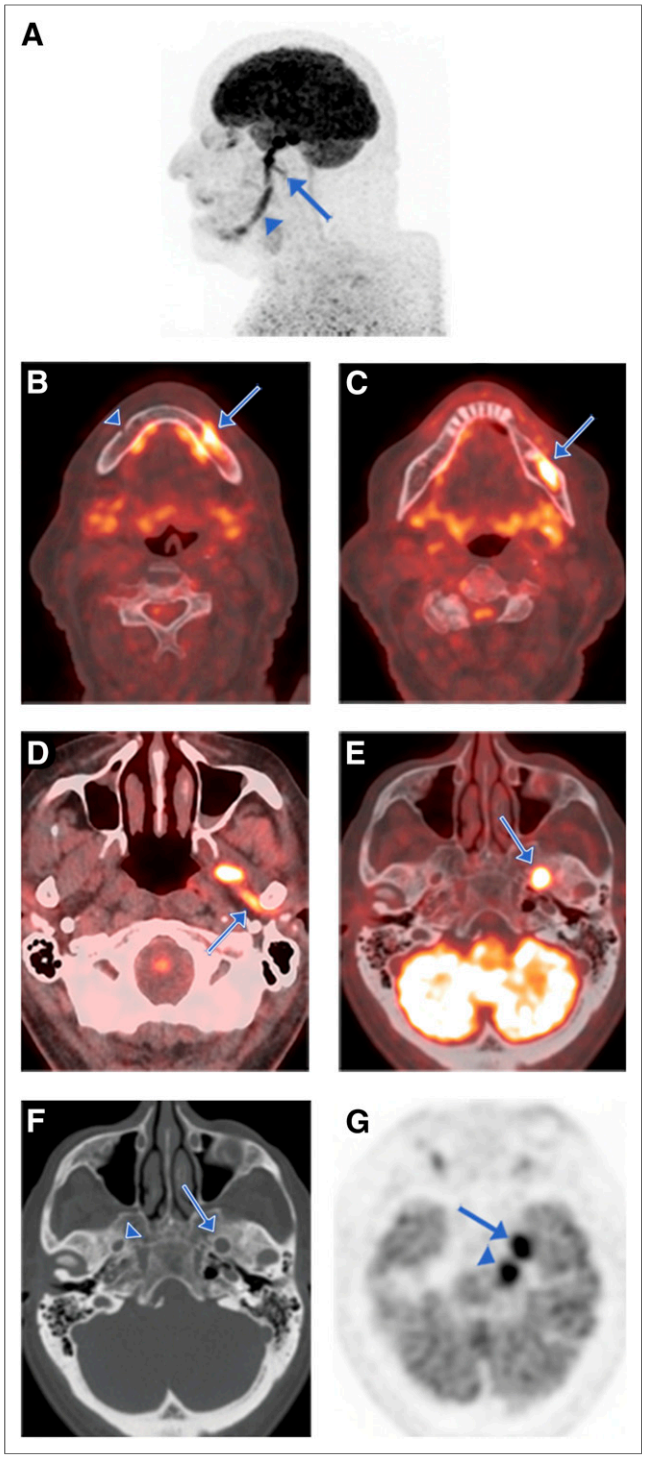

FIGURE 2. CN V3 (mandibular nerve, inferior alveolar and auriculotemporal branch) involvement in patient with recurrent desmoplastic melanoma of left lower lip presenting with left facial numbness. (A) Sagittal maximum-intensity-projection PET image shows ^{18}F-FDG–avid tumor spread along entire course of CN V3 (arrowhead) and along auriculotemporal branch (arrow). (B–G) Axial serial PET/CT and (F) axial CT images show ^{18}F-FDG–avid tumor entry at left mental foramen (arrow, B), in contrast to normal right mental foramen (arrowhead, B) and PNS along inferior alveolar nerve through mandibular canal (arrow, C), along auriculotemporal nerve (arrow, D), and then cephalad through left foramen ovale (arrow, E), which is enlarged (arrow, F) compared with normal contralateral side (arrowhead, F) on CT bone window. (G) Axial PET image shows ^{18}F-FDG–avid tumor spread cephalad to trigeminal ganglion at Meckel cave (arrow) and into cisternal trigeminal nerve in left prepontine cistern (arrowhead). Tumor was deemed inoperable in light of intracranial perineural extension.

interconnect. For example, CN VII fibers communicate with small CN V2 branches in the pterygopalatine ganglion via the greater superficial petrosal nerve; the chorda tympani, a branch of CN VII, joins with the lingual nerve, a branch of CN V3; and CN VII communicates with the auriculotemporal nerve, a branch of CN V3 in the parotid gland (*42–44*). Other regions of CN interconnection include CNs V1 and V2 in the cavernous sinus and CNs V1, V2, and V3 in the Meckel cave (*1,4*).

To interpret an imaging study on a patient with known or suspected head and neck cancer, one should have knowledge of CN anatomy, closely scrutinize the entire course of CNs near the primary tumor, and evaluate the course of the interconnecting CNs. In multiple cranial neuropathies, one should suspect tumor spread to the skull base, PNS to anatomic courses conducive to multiple nerve involvement, or leptomeningeal carcinomatosis (*14*). The continuity between the perineurium and leptomeninges in the intracranial segments of CNs permits leptomeningeal spread of tumor cells (*14*).

CLINICAL FEATURES

Approximately 40% of patients with PNS of tumor in head and neck cancers are asymptomatic (*4*). The signs and symptoms most commonly associated with PNS are facial pain, paresthesia, numbness, and weakness of the muscles of mastication and facial expression, because branches of the trigeminal and facial nerves are the most commonly involved CNs in PNS (*10,26,45*). Such signs and symptoms can direct the interpreting physician's attention to the CNs responsible for the neurologic deficit (Supplemental Table 3).

IMAGING FEATURES

It is well established that imaging plays a key role in assessment and management of head and neck malignancies. Few data exist on the diagnostic performance of ^{18}F-FDG PET/CT for detection of PNS of head and neck cancer, the reason being multifactorial: the interpreting physician's lack of suspicion or of familiarity with the relevant imaging findings, the confounding effects of treatment-related uptake in posttherapy patients, the relatively lower spatial resolution of ^{18}F-FDG PET images, and obscuration of findings by physiologic brain uptake at the skull base. One case-control study reported a PNS detection rate of 100% for ^{18}F-FDG PET/CT, though this is likely an overestimate of the performance in the general clinical setting, as the PET scans in this study were interpreted in light of MRI and tumor board consensus findings of PNS (*46*).

MRI is the modality of choice when evaluating PNS, offering soft-tissue contrast superior to that of CT and fewer artifacts from dental hardware (*26*). The sensitivity and specificity of MRI for detection of PNS is 95%–100% (*5–7*) and 85%, respectively (*5,6*). However, the sensitivity of MRI to demonstrate the full extent of anatomic distribution of PNS is lower, at 63%–89% (*5,7*). In comparison, the sensitivity and specificity of CT for detection of PNS are 88% and 89%, respectively (*6*).

In our experience, both PET and conventional imaging modalities (MRI and CT) should be regarded as complementary in the assessment of PNS, and the full extent of PNS can best be

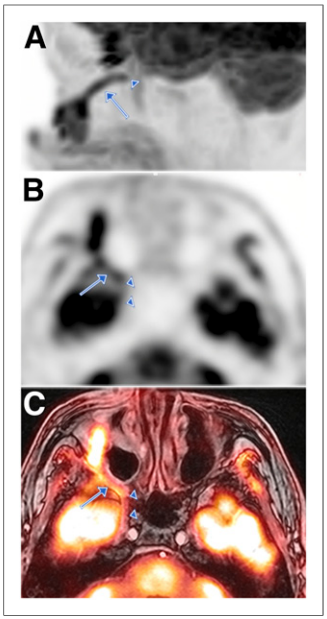

FIGURE 3. CN V2 (maxillary nerve, infraorbital branch) involvement in patient with recurrent squamous cell carcinoma of nose after multiple excisions, including total rhinectomy and postoperative radiotherapy. (A) Sagittal maximum-intensity-projection PET image shows ^{18}F-FDG–avid tumor extension along course of right CN V2, originating from tumor recurrence in right cheek, tracking along infraorbital nerve in infraorbital canal (arrow), and entering inferior orbital fissure into region of right pterygopalatine fossa (arrowhead). (B and C) Axial PET (B) and axial fused PET/MR (C) images show PNS along CN V2 past pterygopalatine fossa (arrow) intracranially through right foramen rotundum (arrowheads) and into inferior cavernous sinus. Tumor management required aggressive local excision.

appreciated with identification of both structural and metabolic imaging findings (Supplemental Table 3).

Primary Imaging Findings

On anatomic imaging, PNS appears as thickening, nodularity, and enhancement of the involved CN (*47,48*). Infiltration or obliteration of fat in the deep spaces of the face and at the skull base foramina is a sensitive indicator of PNS. Enlargement or erosion of the skull base foramina is suggestive of PNS and is better evaluated on CT than on MRI (Fig. 2F) (*47*).

The primary imaging feature of PNS on ^{18}F-FDG PET/CT is linear or curvilinear increased ^{18}F-FDG uptake along the distribution of the CN relative to activity in the surrounding tissue, which may be continuous or discontinuous with the primary tumor (*25*). While interpreting ^{18}F-FDG PET/CT in head and neck cancer, one must assess all 3 standard imaging planes and maximum-intensity-projection PET images to evaluate for PNS. Maximum-intensity-projection technique helps fully visualize the extent of PNS over the nonplanar anatomic course of the involved nerves (Figs. 2A, 3A, and 4C).

Another technique for improved assessment of PNS on ^{18}F-FDG PET/CT is evaluation of the concurrently obtained CT images for the above-described findings. If a recently acquired higher-resolution CT scan (Figs. 5B and 5C) or contrast-enhanced MRI scan (Fig. 3C) is available, retrospective evaluation, correlation, or fusion of the PET images with those scans could also be performed to improve the anatomic localization.

Secondary Imaging Findings

If PNS damages a motor branch of a CN, the denervated musculature undergoes flaccid paresis and eventual atrophy. During the acute phases, there is hyperintense signal and abnormal muscle enhancement on T2-weighted and fat-suppressed contrast-enhanced T1-weighted MR images, respectively, and muscle edema on CT images (*49*). On ^{18}F-FDG PET, one may detect increased ^{18}F-FDG uptake in the affected musculature in the early acute phase that normalizes in the later stages (*50*). In the chronic phase, there is muscle atrophy with decreased ^{18}F-FDG uptake in the affected musculature on PET and volume loss with fatty replacement on CT and MRI (*25,49*). On ^{18}F-FDG PET, a dominant finding may also be increased conspicuity of physiologic or compensatory uptake in the contralateral unaffected musculature, such as in the contralateral tongue or vocal cord in the case of CN XII or X denervation, respectively (*25*).

Potential Imaging Pitfalls

One must also be cautious while reviewing ^{18}F-FDG PET/CT in head and neck cancers. Altered anatomic landmarks after treatment and asymmetric physiologic uptake can often make image interpretation challenging.

The uptake intensity along the nerve course may be subtle, leading to a false-negative scan. Other reasons for a false-negative scan can be improper PET/CT image coregistration because of motion and high adjacent background activity in the brain, which can compromise the evaluation of PNS at the skull base foramina. Also, the partial-volume effect and insufficient spatial resolution for smaller lesions (<1 cm) can limit the sensitivity of PET for PNS detection, particularly for smaller nerve branches, unless there is significantly increased ^{18}F-FDG uptake that contrasts with low background activity (*51*).

False-positive scans can be seen secondary to inflammation from postradiation or postsurgical changes, particularly when the

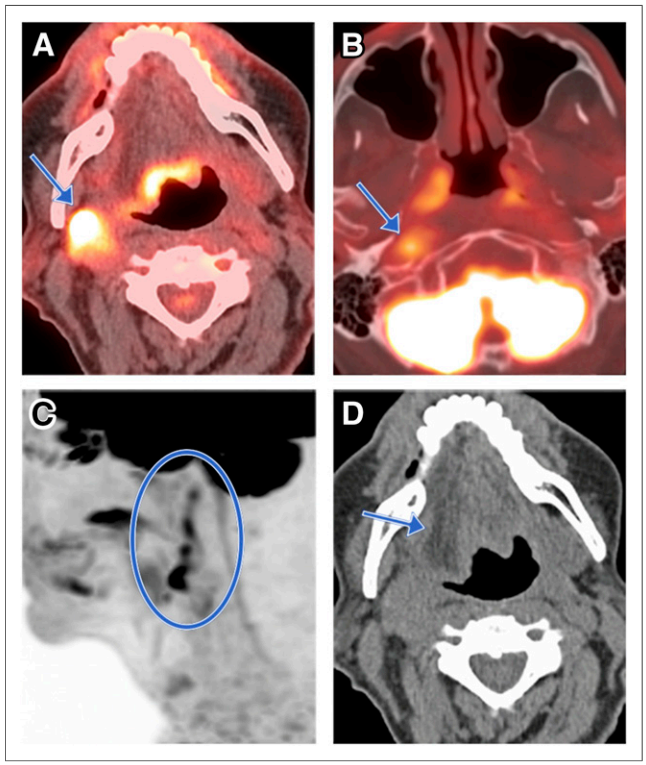

FIGURE 4. CN XII involvement in patient with stage IV metastatic squamous cell carcinoma from unknown primary, presenting with dysphagia and slurred speech. (A and B) Axial PET/CT images show ^{18}F-FDG–avid metastatic tumor in right carotid space (arrow) (A) and ^{18}F-FDG–avid perineural tumor spread along right CN XII superiorly to base of skull just inferior to hypoglossal canal (B). (C) Sagittal maximum-intensity-projection PET image shows course of perineural tumor spread (circle). (D) Axial CT image shows ipsilateral right tongue atrophy with fatty infiltration (arrow) secondary to CN XII palsy. Patient subsequently received palliative radiation therapy of neck mass.

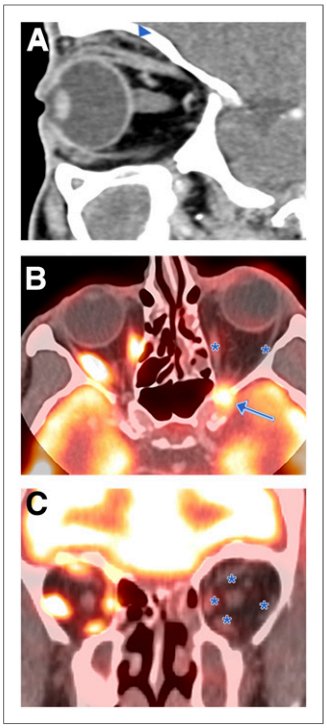

FIGURE 5. CNs V1, II, III, IV, and VI involvement in patient with basal cell carcinoma of left eyebrow after resection, now presenting with progressive loss of left vision and inability to move left eye. Sagittal CT (A), axial ^{18}F-FDG PET/CT (B), and coronal fused PET/CT (C) images of left orbit show cord of soft tissue in superior extraconal space tracking along course of left CN V1 (arrowhead) extending into left orbital apex. Hypermetabolic soft-tissue mass in left orbital apex (arrow) involves CNs II, III, IV, and VI, resulting in vision loss and denervation of left orbital extraocular muscles with atrophy and decreased ^{18}F-FDG uptake in extraocular muscles (asterisks). Further surgical treatment was not pursued, as PNS would have required craniectomy and orbital exenteration.

^{18}F-FDG PET/CT is performed within 1 mo of surgery, chemotherapy, or radiation therapy. The current consensus is that ^{18}F-FDG PET/CT should be deferred until at least 12 wk after chemoradiation therapy to allow resolution of treatment-related changes (*52*). Asymmetric physiologic ^{18}F-FDG uptake in the neck muscles and variable physiologic uptake in normal structures such as masticator muscles, extraocular muscles, and lymphoid tissue such as the Waldeyer ring can also be confounding factors. A review of the CT portion of PET/CT allows correlation of findings with normal anatomic structures, thus reducing the false-positive findings. Some of the mimics of PNS are certain ^{18}F-FDG–avid neurogenic tumors and, rarely, meningioma protruding through the skull base foramina. There are reports of PNS associated with other nonneoplastic diseases such as mucormycosis, invasive aspergillosis, and sinonasal sarcoidosis (*4,18*). Careful assessment of the patient history, physical examination findings, correlative imaging, and histologic information can help avoid such pitfalls.

CN ANATOMY AND PNS IMAGING FEATURES

The trigeminal, facial, and hypoglossal nerves, the most commonly involved CNs with PNS, are described first (Supplemental Figs. 1 and 2), followed by the other less commonly involved CNs.

Trigeminal Nerve (CN V)

The trigeminal nerve emerges from the pons, forms the trigeminal ganglion at the Meckel cave in the middle cranial fossa, and then splits into 3 main divisions: the ophthalmic (CN V1), maxillary (CN V2), and mandibular (CN V3) nerves (*45*).

Mandibular Division of Trigeminal Nerve (CN V3). The mandibular nerve is a mixed sensory and motor nerve, supplying the muscles of mastication (*53*). From the trigeminal ganglion, the mandibular nerve travels inferiorly through the foramen ovale to exit the skull base and enter the masticator space (*45,53*). It then divides into the mostly sensory anterior trunk (deep temporal, lateral pterygoid, masseteric, and buccal nerves) and the mostly motor posterior trunk (auriculotemporal, lingual, and inferior alveolar nerves) (*53*).

Tumors that can spread along the mandibular nerve (CN V3) include lower lip and chin skin cancer (Figs. 2A–2C); neoplasms involving the anterior two thirds of the tongue and the floor of the mouth; periauricular and temporal cutaneous or parotid malignancy; and neoplasms originating from the masticator space, nasopharynx, or oropharynx (*4*).

PNS along the mandibular division can be suspected when abnormal linear uptake on ^{18}F-FDG PET/CT is seen within the mandibular canal along the inferior alveolar nerve (Fig. 2C), on the medial mandibular surface (*3*), or in the masticator space (Fig. 2D). The abnormal uptake can further extend superiorly to reach the foramen ovale (Fig. 2E) or Meckel cave (Fig. 2G). CT or MRI may show enlargement of the neural foramina (mental, mandibular, or ovale) (Fig. 2F). In addition, secondary signs of denervation injury to the ipsilateral masticator muscle may be identified on imaging.

Maxillary Division of Trigeminal Nerve (CN V2). The maxillary nerve, a somatic sensory nerve, travels from the trigeminal ganglion anteriorly across the cavernous sinus and through the foramen rotundum into the pterygopalatine fossa (*53*). It then enters the orbit via the inferior orbital fissure, travels within the infraorbital groove and canal, and then exits the skull through the infraorbital foramen to innervate the facial skin (*54*). From the maxillary nerve also emerge the middle meningeal, zygomatic, and superior alveolar nerves, as well as the pterygopalatine ganglion, where multiple mucosal branches originate (*54*).

PNS along the maxillary nerve most commonly occurs along the mucosal branches by head and neck squamous cell carcinoma or adenoid cystic carcinoma in the oral cavity, pharynx, palate, or sinonasal tract (*26*). Skin malignancy around the cheek, nose, or upper lip, especially squamous cell carcinoma or desmoplastic melanoma, can also spread along the maxillary nerve (*3*).

PNS along the maxillary nerve can be suspected when a mucocutaneous ^{18}F-FDG–avid lesion extends to the infraorbital canal or pterygopalatine fossa and potentially further into the foramen rotundum or the cavernous sinus (Fig. 3). CT or MRI may also identify obliteration of the fat within the pterygopalatine fossa and enlargement of the infraorbital foramen, inferior orbital fissure, or foramen rotundum (Fig. 3).

Ophthalmic Division of Trigeminal Nerve (CN V1). The ophthalmic nerve, a somatic sensory nerve, arises from the trigeminal ganglion in the Meckel cave. It travels anteriorly across the cavernous sinus and splits into the frontal, lacrimal, and nasociliary nerves just before entering the orbit through the superior orbital fissure (*55*). The frontal nerve is the largest branch and exits the orbit to innervate the upper facial skin (*55*).

PNS along the ophthalmic nerve (CN V1) is most commonly caused by skin cancers of the upper face that invade the frontal nerve branches and is less commonly caused by intraorbital or sinonasal neoplasms involving the nasoethmoid complex (*10*).

The small caliber of the CNs within the orbit (except the optic nerve) make it difficult to visualize their involvement on ^{18}F-FDG PET (*25*). Nevertheless, PNS along the ophthalmic nerve can be suspected when a periorbital cutaneous neoplasm makes a seemingly noncontiguous spread to the orbital apex (Fig. 5B). CT/MRI may show direct nerve involvement on high-resolution images (Fig. 5A) or enlargement of the optic canal or superior orbital fissure at the orbital apex. CNs III, IV, and VI may become involved with PNS because they share a common pathway with CN V1 in the cavernous sinus and into the orbit. Decreased ^{18}F-FDG uptake or atrophy of the extraocular muscles (Figs. 5B and 5C) is a useful secondary indicator of PNS.

Facial Nerve (CN VII)

The facial nerve innervates the muscles of facial expression (*56*) and also carries taste afferents from the anterior two thirds of the tongue (*56*). It arises from the brain stem at the lower pons, enters the internal acoustic canal along with the vestibulocochlear nerve, traverses the meatal foramen into the facial canal, and then continues sequentially as the labyrinthine segment, geniculate ganglion, tympanic segment, and mastoid segment before exiting the skull through the stylomastoid foramen (*56*). It then enters the parotid gland and splits into the 5 terminal branches that innervate the muscles of facial expression (*57*). From the geniculate ganglion also emerges the greater superficial petrosal nerve carrying the parasympathetic fibers, joining branches of the maxillary nerve (CN V2) at the pterygopalatine ganglion (*57*).

PNS along the facial nerve most commonly occurs in primary parotid malignancy or through neoplasia from the adjacent skin invading the parotid gland (*1,26*). Tumor can spread cephalad from the parotid gland, with abnormal ^{18}F-FDG activity at the stylomastoid foramen and mastoid segment of the temporal bone (Fig. 6) or stylomastoid foramen enlargement on anatomic imaging raising suspicion of PNS. Another commonly involved neural pathway is along the greater superficial petrosal nerve by a neoplasm reaching the pterygopalatine ganglion, such as a hard-palate adenoid cystic carcinoma (*10*).

Hypoglossal Nerve (CN XII)

The hypoglossal nerve controls the muscles of the tongue (*58*). Emerging from the medulla, the hypoglossal nerve travels through the hypoglossal canal and down the carotid space (*58*). At the level of the angle of the mandible, it turns anteriorly to reach the muscles of the tongue (*58*). The cervical course of the hypoglossal nerve in the carotid space is near CNs IX, X, and XI.

PNS along the hypoglossal nerve is most commonly caused by posterolateral extension of nasopharyngeal carcinoma (*10*). There may also be retrograde spread from a tongue base or sublingual space malignancy (*57,58*) or a metastatic carotid space tumor, shown as an abnormally ^{18}F-FDG–avid lesion tracking superiorly along the carotid space to the hypoglossal canal on PET/CT (Fig. 4). Potential secondary imaging findings of PNS along the hypoglossal nerve include decreased ^{18}F-FDG activity and atrophy or fatty replacement of the ipsilateral tongue as a late stage of denervation injury on ^{18}F-FDG PET/CT (Fig. 4D) and MRI, as well as hypoglossal canal enlargement on anatomic imaging.

Olfactory Nerve (CN I)

The olfactory nerve carries the sense of smell from the nasal mucosa (*59*). The olfactory nerve refers to bundles of axons that originate from the olfactory bulb and pass through the numerous olfactory foramina in the cribriform plate of the ethmoid bone (*59*). Although direct visualization of the olfactory nerve is beyond the resolution of ^{18}F-FDG PET (*25*), PNS should be suspected when the cribriform plate is involved with lesions in the superior sinonasal and anterior cranial fossa region by tumors such as esthesioneuroblastoma, sinonasal squamous cell carcinoma, and melanoma (Supplemental Fig. 3).

Optic, Oculomotor, Trochlear, and Abducens Nerves (CNs II, III, IV, and VI)

The optic nerve originates from the optic chiasm and enters the orbit via the optic canal, innervating the retina to carry visual sensory information (*59*). The oculomotor, trochlear, and abducens nerves control the extraocular muscles and arise from the brain stem. PNS along CN V1 can involve any of these other CNs in the orbit because they share a similar course along the cavernous sinus into the superior orbital fissure and the orbit. Focally increased ^{18}F-FDG uptake in the orbital apex or cavernous sinus with secondary findings of extraocular muscle atrophy should raise suspicion of CN III, IV or VI involvement in a patient with a periorbital neoplasm (Fig. 5).

Vestibulocochlear Nerve (CN VIII)

The vestibulocochlear nerve is responsible for sensations of hearing and rotational or linear acceleration (*60*). This nerve emerges from the pontomedullary junction and enters the internal acoustic canal alongside the facial nerve and innervates the cochlear and vestibular apparatus within the petrous part of the temporal bone (*60*).

Perineural involvement of the vestibulocochlear nerve can occur when PNS of head and neck cancer along the facial nerve has extended cephalad past the geniculate ganglion into its canalicular segment, where CN VII and CN VIII are in close proximity. Linearly increased uptake in the internal acoustic canal on ^{18}F-FDG PET/CT, or destruction of the bony labyrinth or enlargement of the internal acoustic canal on CT or MRI, should also raise suspicion of vestibulocochlear nerve involvement in a patient with facial nerve PNS presenting with new symptoms of hearing loss or imbalance (Supplemental Fig. 4).

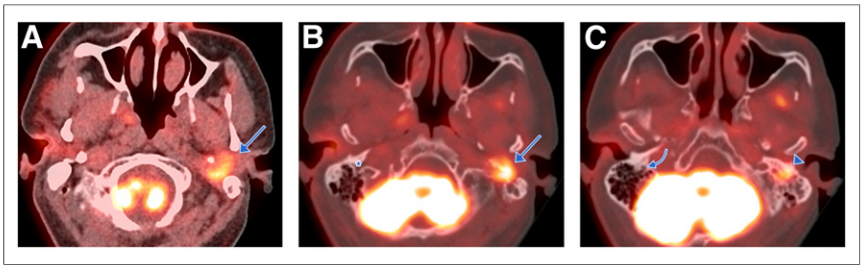

FIGURE 6. CN VII involvement in patient with myoepithelial carcinoma of left parotid gland after parotidectomy and chemoradiation, now with tumor recurrence and left-sided preauricular pain, facial droop exacerbation, and metallic taste. (A) Axial PET/CT image shows ^{18}F-FDG–avid mass representing local tumor recurrence deep to parotidectomy bed and anterior to left mastoid tip (arrow). (B and C) Axial PET/CT images show ^{18}F-FDG uptake extending cephalad from parotid space through stylomastoid foramen (arrow) into facial canal in left mastoid temporal bone (arrowhead), representing PNS along mastoid segment of CN VII, in comparison to contralateral normal stylomastoid foramen (asterisk) and facial canal (curved arrow). Recurrent tumor had partial treatment response with stereotactic radiosurgery.

Glossopharyngeal, Vagus, and Accessory Nerves (CNs IX, X, and XI)

The glossopharyngeal nerve supplies efferent fibers to the stylopharyngeus muscle and parotid gland while also receiving sensory input from the pharyngeal mucosa, palatine tonsil, carotid body, and posterior third of the tongue (*61*). The vagus nerve carries motor fibers to the muscles of the larynx and pharynx responsible for speech and swallowing, along with sensory fibers from the same areas (*61*). It also provides visceral sensory and parasympathetic motor

innervation to the thorax and abdomen (*61*). The accessory nerve innervates the sternocleidomastoid and trapezius muscles (*61*).

The glossopharyngeal, vagus, and accessory nerves share their anatomic course through the jugular foramen at the skull base and down the carotid space (*59,61*). Therefore, a head and neck neoplasm extending to the carotid space can subsequently spread variably along these 3 CNs to reach the jugular foramen, visible as focal or linear abnormal uptake along their course in the lateral neck and jugular foramen on ^{18}F-FDG PET (Supplemental Fig. 5). There may be enhancement along the nerve course on T1-weighted contrast-enhanced MRI and widening or destructive bony changes in the jugular foramen on CT. End-organ dysfunction will result in paralysis of pharyngeal and soft-palate muscles secondary to involvement of the glossopharyngeal and vagus nerves, vocal cord paralysis with involvement of recurrent laryngeal branch of the vagus nerve (Supplemental Fig. 6A), and paralysis of the sternocleidomastoid and trapezius muscles with accessory nerve involvement (Supplemental Fig. 6B).

CONCLUSION

PNS, an important neoplastic feature with an impact on prognosis and management, needs to be considered and recognized on imaging. ^{18}F-FDG PET can identify PNS of head and neck malignancies along the CNs. Correlation or fusion of PET with CT or MRI improves assessment of both the presence and the extent of PNS. Knowledge of the imaging findings and associated neuroanatomy, further processing of the images, and review of the clinical context can improve interpretation of suspected cases of PNS. The advent of PET/MR in clinical practice may further enhance detection of PNS in head and neck tumors.

REFERENCES

1. Ginsberg LE. Imaging of perineural tumor spread in head and neck cancer. *Semin Ultrasound CT MR.* 1999;20:175–186.
2. Subramaniam RM, Truong M, Peller P, Sakai O, Mercier G. Fluorodeoxyglucose-positron-emission tomography imaging of head and neck squamous cell cancer. *AJNR Am J Neuroradiol.* 2010;31:598–604.
3. Paes FM, Singer AD, Checkver AN, Palmquist RA, De La Vega G, Sidani C. Perineural spread in head and neck malignancies: clinical significance and evaluation with ^{18}F-FDG PET/CT. *Radiographics.* 2013;33:1717–1736.
4. Gandhi D, Gujar S, Mukherji SK. Magnetic resonance imaging of perineural spread of head and neck malignancies. *Top Magn Reson Imaging.* 2004;15:79–85.
5. Baulch J, Gandhi M, Sommerville J, Panizza B. 3T MRI evaluation of large nerve perineural spread of head and neck cancers. *J Med Imaging Radiat Oncol.* 2015;59:578–585.
6. Hanna E, Vural E, Prokopakis E, Carrau R, Snyderman C, Weissman J. The sensitivity and specificity of high-resolution imaging in evaluating perineural spread of adenoid cystic carcinoma to the skull base. *Arch Otolaryngol Head Neck Surg.* 2007;133:541–545.
7. Nemzek WR, Hecht S, Gandour-Edwards R, Donald P, McKennan K. Perineural spread of head and neck tumors: how accurate is MR imaging? *AJNR Am J Neuroradiol.* 1998;19:701–706.
8. Brown IS. Pathology of perineural spread. *J Neurol Surg B Skull Base.* 2016;77:124–130.
9. Marchesi F, Piemonti L, Mantovani A, Allavena P. Molecular mechanisms of perineural invasion, a forgotten pathway of dissemination and metastasis. *Cytokine Growth Factor Rev.* 2010;21:77–82.
10. Maroldi R, Farina D, Borghesi A, Marconi A, Gatti E. Perineural tumor spread. *Neuroimaging Clin N Am.* 2008;18:413–429.
11. Roh J, Muelleman T, Tawfik O, Thomas SM. Perineural growth in head and neck squamous cell carcinoma: a review. *Oral Oncol.* 2015;51:16–23.
12. Blanchard P, Baujat B, Holostenco V, et al. Meta-analysis of chemotherapy in head and neck cancer (MACH-NC): a comprehensive analysis by tumour site. *Radiother Oncol.* 2011;100:33–40.
13. Chirilă M, Bolboaca SD, Cosgarea M, Tomescu E, Muresan M. Perineural invasion of the major and minor nerves in laryngeal and hypopharyngeal cancer. *Otolaryngol Head Neck Surg.* 2009;140:65–69.
14. Dunn M, Morgan MB, Beer TW. Perineural invasion: identification, significance, and a standardized definition. *Dermatol Surg.* 2009;35:214–221.
15. Alam M, Ratner D. Cutaneous squamous-cell carcinoma. *N Engl J Med.* 2001;344:975–983.
16. Hassanein AM, Proper SA, Depcik-Smith ND, Flowers FP. Peritumoral fibrosis in basal cell and squamous cell carcinoma mimicking perineural invasion: potential pitfall in Mohs micrographic surgery. *Dermatol Surg.* 2005;31:1101–1106.
17. McHugh CH, Roberts DB, El-Naggar AK, et al. Prognostic factors in mucoepidermoid carcinoma of the salivary glands. *Cancer.* 2012;118:3928–3936.
18. Ronaghy A, Yaar R, Goldberg LJ, Mahalingam M, Bhawan J. Perineural involvement: what does it mean? *Am J Dermatopathol.* 2010;32:469–476.
19. Yu JB, Blitzblau RC, Patel SC, Decker RH, Wilson LD. Surveillance, Epidemiology, and End Results (SEER) database analysis of microcystic adnexal carcinoma (sclerosing sweat duct carcinoma) of the skin. *Am J Clin Oncol.* 2010;33:125–127.
20. Chang PC, Fischbein NJ, McCalmont TH, et al. Perineural spread of malignant melanoma of the head and neck: clinical and imaging features. *AJNR Am J Neuroradiol.* 2004;25:5–11.
21. Barrett AW, Speight PM. Perineural invasion in adenoid cystic carcinoma of the salivary glands: a valid prognostic indicator? *Oral Oncol.* 2009;45:936–940.
22. Naylor E, Sarkar P, Perlis CS, Giri D, Gnepp DR, Robinson-Bostom L. Primary cutaneous adenoid cystic carcinoma. *J Am Acad Dermatol.* 2008;58:636–641.
23. Dores GM, Huycke MM, Devesa SS, Garcia CA. Primary cutaneous adenoid cystic carcinoma in the United States: incidence, survival, and associated cancers, 1976 to 2005. *J Am Acad Dermatol.* 2010;63:71–78.
24. Balamucki CJ, Mancuso AA, Amdur RJ, et al. Skin carcinoma of the head and neck with perineural invasion. *Am J Otolaryngol.* 2012;33:447–454.
25. Raslan OA, Muzaffar R, Shetty V, Osman MM. Image findings of cranial nerve pathology on [^{18}F]-2-deoxy-D-glucose (FDG) positron emission tomography with computerized tomography (PET/CT): a pictorial essay. *Cancer Imaging.* 2015;15:20.
26. Amit M, Eran A, Billan S, et al. Perineural spread in noncutaneous head and neck cancer: new insights into an old problem. *J Neurol Surg B Skull Base.* 2016;77:86–95.
27. Bakst RL, Wong RJ. Mechanisms of perineural invasion. *J Neurol Surg B Skull Base.* 2016;77:96–106.
28. Bakst RL, Xiong H, Chen CH, et al. Inflammatory monocytes promote perineural invasion via CCL2-mediated recruitment and cathepsin B expression. *Cancer Res.* 2017;77:6400–6414.
29. Ohsie SJ, Sarantopoulos GP, Cochran AJ, Binder SW. Immunohistochemical characteristics of melanoma. *J Cutan Pathol.* 2008;35:433–444.
30. Amatu A, Sartore-Bianchi A, Siena S. NTRK gene fusions as novel targets of cancer therapy across multiple tumour types. *ESMO Open.* 2016;1:e000023.
31. Drilon A, Laetsch TW, Kummar S, et al. Efficacy of larotrectinib in TRK fusion-positive cancers in adults and children. *N Engl J Med.* 2018;378:731–739.
32. Fagan JJ, Collins B, Barnes L, D'Amico F, Myers EN, Johnson JT. Perineural invasion in squamous cell carcinoma of the head and neck. *Arch Otolaryngol Head Neck Surg.* 1998;124:637–640.
33. Cracchiolo JR, Xu B, Migliacci JC, et al. Patterns of recurrence in oral tongue cancer with perineural invasion. *Head Neck.* 2018;40:1287–1295.
34. Vrielinck LJ, Ostyn F, van Damme B, van den Bogaert W, Fossion E. The significance of perineural spread in adenoid cystic carcinoma of the major and minor salivary glands. *Int J Oral Maxillofac Surg.* 1988;17:190–193.
35. Williams LS, Mancuso AA, Mendenhall WM. Perineural spread of cutaneous squamous and basal cell carcinoma: CT and MR detection and its impact on patient management and prognosis. *Int J Radiat Oncol Biol Phys.* 2001;49:1061–1069.
36. Warren TA, Panizza B, Porceddu SV, et al. Outcomes after surgery and postoperative radiotherapy for perineural spread of head and neck cutaneous squamous cell carcinoma. *Head Neck.* 2016;38:824–831.
37. Palejwala SK, Barry JY, Rodriguez CN, Parikh CA, Goldstein SA, Lemole GM Jr. Combined approaches to the skull base for intracranial extension of tumors via perineural spread can improve patient outcomes. *Clin Neurol Neurosurg.* 2016;150:46–53.
38. NCCN clinical practice guidelines in oncology: head and neck cancers (version 1.2018). National Comprehensive Cancer Network website. https://www.nccn.org/professionals/physician_gls/pdf/head-and-neck.pdf. Updated June 20, 2018. Accessed October 9, 2018.
39. NCCN clinical practice guidelines in oncology: melanoma (version 2.2018). National Comprehensive Cancer Network website. https://www.nccn.org/professionals/physician_gls/PDF/melanoma.pdf. Updated July 12, 2018. Accessed October 9, 2018.

40. NCCN clinical practice guidelines in oncology: squamous cell skin cancer (version 2.2018). National Comprehensive Cancer Network website. https://www.nccn.org/professionals/physician_gls/pdf/squamous.pdf. Updated August 31, 2018. Accessed October 9, 2018.
41. NCCN clinical practice guidelines in oncology: basal cell skin cancer (version 1.2018). National Comprehensive Cancer Network website. https://www.nccn.org/professionals/physician_gls/pdf/nmsc.pdf. Updated August 31, 2018. Accessed October 9, 2018.
42. Schmalfuss IM, Tart RP, Mukherji S, Mancuso AA. Perineural tumor spread along the auriculotemporal nerve. *AJNR Am J Neuroradiol.* 2002;23:303–311.
43. Ginsberg LE, De Monte F, Gillenwater AM. Greater superficial petrosal nerve: anatomy and MR findings in perineural tumor spread. *AJNR Am J Neuroradiol.* 1996;17:389–393.
44. Bagatin M, Orihovac Z, Mohammed AM. Perineural invasion by carcinoma of the lower lip. *J Craniomaxillofac Surg.* 1995;23:155–159.
45. Gaddikeri S, Bhrany A, Anzai Y. Perineural invasion of skin cancers in the head and neck: an uncommon phenomenon revisited. *Otolaryngology.* 2014;4:2.
46. Dercle L, Hartl D, Rozenblum-Beddok L, et al. Diagnostic and prognostic value of ^{18}F-FDG PET, CT, and MRI in perineural spread of head and neck malignancies. *Eur Radiol.* 2018;28:1761–1770.
47. Caldemeyer KS, Mathews VP, Righi PD, Smith RR. Imaging features and clinical significance of perineural spread or extension of head and neck tumors. *Radiographics.* 1998;18:97–110.
48. Ginsberg LE. MR imaging of perineural tumor spread. *Neuroimaging Clin N Am.* 2004;14:663–677.
49. Russo CP, Smoker WR, Weissman JL. MR appearance of trigeminal and hypoglossal motor denervation. *AJNR Am J Neuroradiol.* 1997;18:1375–1383.
50. Lee SH, Seo HG, Oh BM, Choi H, Cheon GJ, Lee SU. Increased ^{18}F-FDG uptake in the trapezius muscle in patients with spinal accessory neuropathy. *J Neurol Sci.* 2016;362:127–130.
51. Fukui MB, Blodgett TM, Snyderman CH, et al. Combined PET-CT in the head and neck: part 2. Diagnostic uses and pitfalls of oncologic imaging. *Radiographics.* 2005;25:913–930.
52. Sheikhbahaei S, Taghipour M, Ahmad R, et al. Diagnostic accuracy of follow-up FDG PET or PET/CT in patients with head and neck cancer after definitive treatment: a systematic review and meta-analysis. *AJR.* 2015;205:629–639.
53. Rodella LF, Buffoli B, Labanca M, Rezzani R. A review of the mandibular and maxillary nerve supplies and their clinical relevance. *Arch Oral Biol.* 2012;57:323–334.
54. Shankland WE. The trigeminal nerve. Part III: the maxillary division. *Cranio.* 2001;19:78–83.
55. Shankland WE. The trigeminal nerve. Part II: the ophthalmic division. *Cranio.* 2001;19:8–12.
56. Phillips CD, Bubash LA. The facial nerve: anatomy and common pathology. *Semin Ultrasound CT MR.* 2002;23:202–217.
57. Moonis G, Cunnane MB, Emerick K, Curtin H. Patterns of perineural tumor spread in head and neck cancer. *Magn Reson Imaging Clin N Am.* 2012;20:435–446.
58. Roncallo F, Turtulici I, Arena E, et al. Unilateral hypoglossal neuropathy: a pictorial essay. *Neuroradiol J.* 1998;11:849–864.
59. Morani AC, Ramani NS, Wesolowski JR. Skull base, orbits, temporal bone, and cranial nerves: anatomy on MR imaging. *Magn Reson Imaging Clin N Am.* 2011;19:439–456.
60. Khan S, Chang R. Anatomy of the vestibular system: a review. *NeuroRehabilitation.* 2013;32:437–443.
61. Larson TC, Aulino JM, Laine FJ. Imaging of the glossopharyngeal, vagus, and accessory nerves. *Semin Ultrasound CT MR.* 2002;23:238–255.